31.1: *Invited Paper:* The Spatial Standard Observer: A Human Vision Model for Display Inspection

Andrew B. Watson
NASA Ames Research Center, MS 262-2, Moffett Field, CA 94035-1000

Abstract

We have developed a simple model of human sensitivity to spatial contrast patterns, called the Spatial Standard Observer. This model can be applied to numerous problems in display inspection and measurement. In this paper I describe two examples: measurement of mura and measurement of motion blur. In each case the Spatial Standard Observer can provide a measure of the artifact in units of just-noticeable differences.

Objective and Background:

We are in the midst of an explosive growth in digital display technology applications, and a consequent growth in the market for digital flat panel displays of all sizes. In 2005 worldwide shipments of LCD desktop monitors will exceed 100 million, LCD-TV panel shipments will rise to over 20 million, and laptop displays will amount to 60 million. This nearly 200 million unit figure does not include plasma, OLED, and many other flat panel display technologies. Total production of flat panel displays, both small and large, is expected to continue to increase in the coming years.

During manufacture, flat panel displays are manually inspected for visual defects. During design or evaluation, displays are measured with instruments to quantify their visual quality. In both of these cases, a vision model can be of value: in the first case to automate the inspection process; and in the second case to provide measurements that more closely mimic the judgments of the human eye.

We have developed a simple model of human visual sensitivity to spatial contrast that can be used in display inspection and measurement applications.

Spatial Standard Observer

Definition

The Spatial Standard Observer (SSO) is a simplified model of human visual sensitivity to spatial patterns. It is a simple tool for measuring the visibility of foveal spatial patterns, or the discriminability of two patterns. It operates on a pair of images (test and reference), one of which may be a uniform field. The images are defined as digital grayscale images, with an arbitrary size in pixels but subtending 2 degrees or less. Larger images can be handled with suitable extensions to the metric. The images are assumed to be viewed at a specific viewing distance, and the pixels have a known relation to luminance. The output of the metric is a measure of the visibility of the difference between test and reference images, in units of just-noticeable difference (JND).

Development

The SSO was based largely on models developed to account for the ModelFest dataset. This set of contrast detection thresholds for 43 foveal stimuli was collected from 16 observers in 10 labs in order to test and calibrate models of spatial vision [1-3]. By evaluating the fit of a model containing multiple serial components we were able to identify which components were necessary, and to estimate relevant parameters.

The resulting model includes a contrast sensitivity function, an oblique effect, a spatial aperture, and Minkowski pooling. Extensions of the basic model incorporate spatial masking and viewing of larger images. The overall fit of the model is shown in Figure 1.

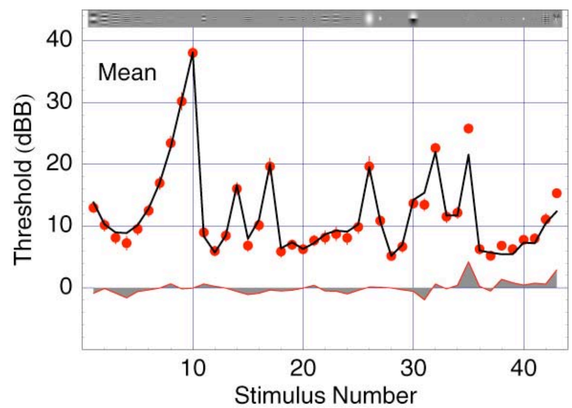

Figure 1. Mean observer data from the ModelFest experiment (red points) and fit of the Spatial Standard Observer (black curve). The vertical axis is in units of log contrast energy. The horizontal axis indicates ModelFest stimulus number. Miniature versions of the stimuli are shown at the top of the figure.

We considered a wide variety of formulae for the contrast sensitivity function, and identified a number that fit very well, and about equally well. Among these, one CSF fits the best. This is the one we call HPmH. It is a hyperbolic secant whose scaled frequency is raised to the power p, minus a second hyperbolic secant with a different frequency scaling:

$$S_{HPmH}\left(f;f_0,f_1,a,p\right)=\operatorname{sech}\left[\left(f/f_0\right)^p\right]-a\operatorname{sech}\left[f/f_1\right]$$

where f is radial spatial frequency in cycles/deg, and f_0, f_1, a, and p are parameters. Combined with an oblique effect, this formula results in the two-dimensional CSF pictured in Figure 2.

The SSO produces measurements in units of JND (Just Noticeable Difference). This is a standard measure in the science of subjective measurement; 1 JND indicates that a signal is just visible.

Mura Inspection

While flat panel display manufacturing is highly automated, most flat panels are examined for defects by human inspectors. This inspection stage is slow and costly, and becomes more difficult as panel sizes increase. Reliability and consistency of inspection are also generally unknown.

 ISSN0006-0966X/06/3702-1312-$1.00+.00

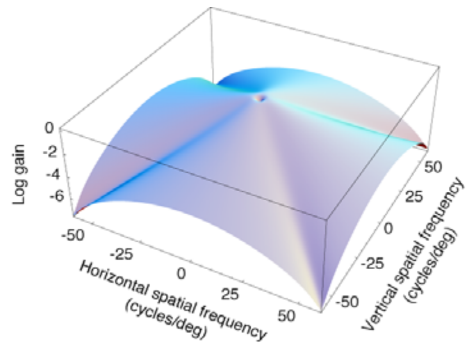

Figure 2. Contrast sensitivity function of the spatial standard observer.

One important category of defect is called "mura," derived from the Japanese word for blemish[4]. Mura are typically low-contrast defects that are larger than a single pixel, and that are visible when the display is driven at a uniform value.

There have been previous efforts to define and quantify mura [4][5]. However, these definitions do not provide a clear method for measuring real mura, in part because the definitions are normative, and do not provide general measurement methods.

In order to automate the process of display inspection, it is necessary to quantify the visibility, to a human, of the defect. This requires a calibrated model of human sensitivity to spatial patterns. We have provided such a model in the form of the Spatial Standard Observer. In addition, we have tailored the SSO to the display inspection application.

There have also been previous efforts to apply vision models [6], or parametric methods [7] to mura inspection. However, we believe the SSO provides a more accurate and general approach because it is based on a validated general model of human vision.

In the case of mura detection, a single image of the display under test is acquired. This image is first preprocessed to remove signals that are not of interest. It may also be cropped and down-sampled. A reference image is then created from this image by removing mura-like signals. Test and reference images are then compared and their difference measured. The basic steps in the SSO analysis of mura are depicted in Figure 3.

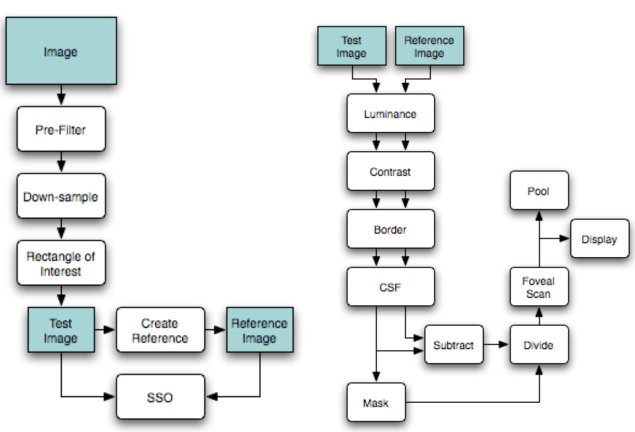

Figure 3. A. Preprocessing of the captured display image and creation of the reference image. B. Application of Spatial Standard Observer to mura measurement.

The SSO produces measurements in units of JND. A mura with a measure of 1 JND would be just barely detectable, while a mura with a measure of 4 JND would be quite detectable.

In a typical mode of operation, the SSO produces both an image showing the location of the mura, as well as a peak JND measure, defining the worst artifact in the image. Other products are possible.

An example is shown in Figure 4. On the left is an image captured from a 17 inch LCD panel. The primary defect here is a bright blob in the upper right of the display. On the right is the SSO output, shown as an image, and thresholded at 2 JND (typically displays have many low-level artifacts that are not visually significant, and thresholding removes them from the output visualization). Measurements of this sort can be easily used for grading, selecting, or rejecting displays, as well as identifying the location of the major artifacts.

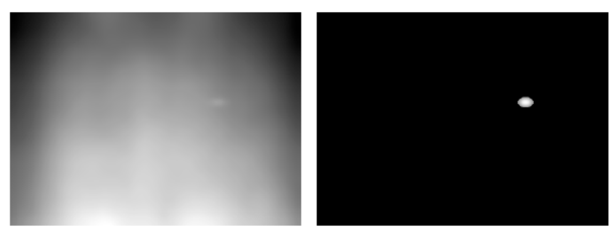

Figure 4. Example of SSO mura measurement. The left image is a capture of a 17 LCD panel. The right image shows the SSO output image, thresholded at 2 JND. The peak value is 4.1 JND.

Motion Blur

Current LCD displays excel in many respects, but remain inferior to the best CRT displays in their temporal response. This relatively slow response results in a blurring of rapidly moving edges. This motion blur can be measured with a pursuit camera system, to provide an image as seen by an eye tracking the moving edge [8]. Here we show that for most purposes the motion blur can be derived mathematically from the temporal step response function of the display, obviating the need for a pursuit camera. We then show that the blurred edge can be analyzed by the spatial standard observer to report a measure of the motion blur artifact in JNDs.

Computing Motion Blur

We begin by defining a negative step response function, which describes the change in luminance over time following a change from white to black. We write this as $T(t)$. As an illustrative example, we consider a change from light to dark that follows an exponential decay:

$$\begin{aligned} T(t) &= 1 - \mathrm{Exp}(-t/\tau) \quad t > 0 \\ &= 1 \quad t < 0 \end{aligned} \tag{1}$$

This example is plotted here for $\tau = 1$.

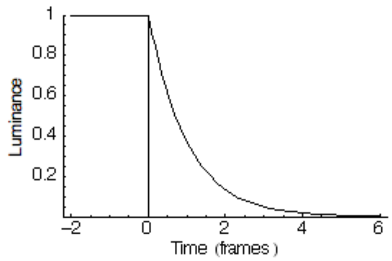

Figure 5. An exponential transition function with a time constant of $\tau = 1$ frame.

Now we consider the luminance along a row of pixels as an edge is moved to the right at a speed of r pixels/frame,

$$E(x,t,r) = T(t - F(x/r)) \tag{2}$$

where F is the floor function, which returns the largest integer less than its argument. This edge function is pictured for our example of T and for $r = 2$

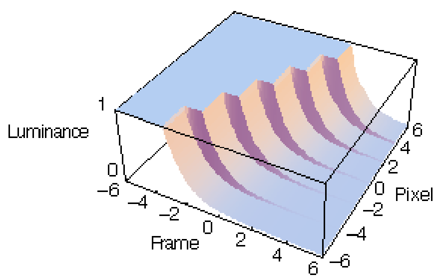

Figure 6. The edge function for an edge speed of $r = 2$ pixels/frame and an exponential transition function with a time constant of $\tau = 1$ frame (Figure 5).

If we now track the moving edge with our eye or a camera, moving at a constant speed r, the result is a stabilized edge given by

$$\begin{aligned} S(x,t,r) &= E(x+rt,t,r) \\ &= T\left(t - F\left(t + \frac{x}{r}\right)\right) \end{aligned} \tag{3}$$

In effect the space-time image shown above is sheared in the space domain. This is pictured in Figure 7.

At any fixed value of x, this function is periodic in time with period 1 frame. An example at $x = 0$ is pictured in Figure 8.

To a first approximation, the eye acts as an integrator over time. Since the luminance at any point in space is periodic over time with period of one frame, we can integrate over a single frame. Thus the expression for the apparent spatial edge is

$$\begin{aligned} A(x,r) &= \int_0^1 S(x,t,r)dt \\ &= \int_0^1 T\left(t - F\left(t + \frac{x}{r}\right)\right)dt \end{aligned} \tag{4}$$

Note that because the integrand is periodic, the limits of

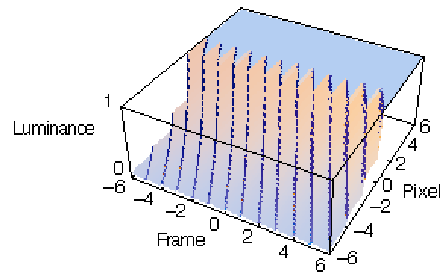

Figure 7. Stabilized edge function for an exponential transition function with a time constant of τ = 1 frame (Figure 1).

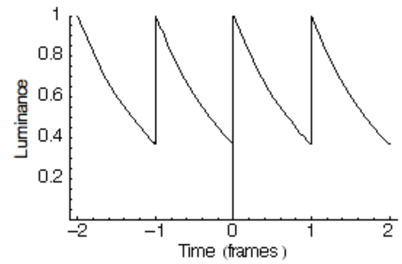

Figure 8. The stabilized edge viewed at $x = 0$.

integration can be any interval of length 1. Specifically, we consider the interval $\{-x/r, 1-x/r\}$,

$$\begin{aligned} A(x,r) &= \int_{-\frac{x}{r}}^{1-\frac{x}{r}} T\left(t - F\left(t + \frac{x}{r}\right)\right)dt \\ &= \int_{-\frac{x}{r}}^{1-\frac{x}{r}} T(t)dt \end{aligned} \tag{5}$$

The simplification occurs because the floor function is zero over the interval in question.

Finally, we note that this definite integral can be converted to an indefinite integral by multiplying by a shifted unit pulse P,

$$A(x,r) = \int_{-\infty}^{\infty} P\left(t - \frac{x}{r}\right) T(t)dt \tag{6}$$

This last expression is recognizable as a convolution,

$$A(x,r) = T\left(-\frac{x}{r}\right) * P\left(\frac{x}{r}\right) \tag{7}$$

Thus we arrive at the following result: the apparent edge is the convolution of a pulse of width one frame and the transition function, both scaled by the speed r. The following is an illustration of the apparent edge, again for the example of $r = 2$.

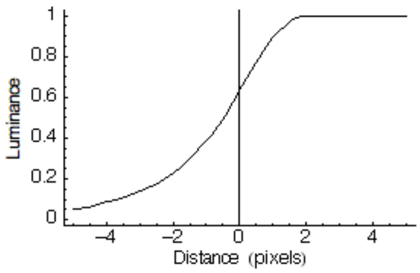

Figure 9. The apparent edge function for an exponential transition function with a time constant of $\tau = 1$ frame (Figure 1), and a speed of $r = 2$ pixels/frame.

Because this function scales with edge speed *r*, it is better considered a function of time. This is achieved by setting $r = 1$, and expressing the result in frames. We will call this the temporal edge blur. The amount of spatial blur is then easily derived by scaling this temporal edge blur by the speed in pixels/frame. Here is the canonical function for the example function *T* that we have used so far. It is simply the transition function convolved with a unit pulse.

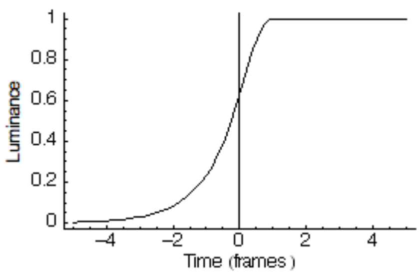

Figure 10. The temporal edge blur for an exponential transition function with a time constant of $\tau = 1$ frame (Figure 1).

At this point we note that this general analysis can be extended to deal with arbitrary positive or negative step responses, with a bright edge, a gray edge, a bright or dark line, or an arbitrary image, and that it can also deal with manipulations such as overdrive, black insertion, and strobing backlights.

Computing Blur Visibility

We have shown how to compute the apparent edge produced by a particular transition function and edge speed, but we do not yet know whether a particular apparent edge will appear sharp – that is, will it be discriminable from a sharp edge. There are several possible methods to transform the apparent edge into a useful measure of artifact visibility. In this section we describe a metric that we call the Visible Motion Blur.

One problem with existing blur width measures such as MPRT, BET, and EBET is that they do not take into account the possibly complex shape of the temporal step response. The Visible Motion Blur provides a metric that is a more general measure of the departure from a perfect edge.

This measure is computed by the Spatial Standard Observer, and is based on the visibility of the difference between an ideal edge and the apparent edge. We compute the difference between these two edges, and then filter the result with the SSO spatial CSF (Figure 2).

An example is illustrated in Figure 11: on the left we show the difference between the ideal edge and the apparent edge; on the right the difference has been filtered by the CSF.

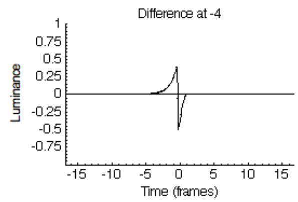

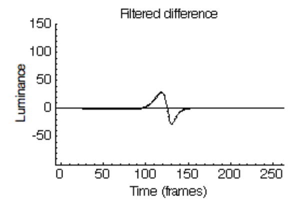

Figure 11. Difference between an ideal edge and the apparent edge (left), and the filtered difference (right). The results are for an edge that has been shifted in order to minimize the pooled error between the two functions.

The filtered difference is then windowed and pooled non-linearly over space to yield a visibility measure in JNDs, the Visible Motion Blur. The resulting VMB measure can be used to specify the effects of step response, viewing distance, and speed of edge motion.

Impact:

The ability to automatically measure mura in flat panel displays will improve the efficiency and thus lower the cost of automated manufacture of large flat panel displays. Ability to simulate motion blur from temporal response will obviate the need for a pursuit camera in most cases. A perceptually based measure of motion blur will allow rational design and selection of displays and display technologies.

References

[1] T. Carney, C. W. Tyler, A. B. Watson, W. Makous, B. Beutter, C.-C. Chen, A. M. Norcia, and S. A. Klein, "Modelfest: year one results and plans for future years," *Human Vision, Visual Processing, and Digital Display IX*, vol. 3959, pp. 140-151, 2000.

[2] A. B. Watson, "Visual detection of spatial contrast patterns: Evaluation of five simple models," *Optics Express*, vol. 6, pp. 12-33, 2000.

[3] A. B. Watson and A. J. Ahumada, Jr "A standard model for foveal detection of spatial contrast," *Journal of Vision*, vol. 5, pp. 717-740, 2005. http://journalofvision.org/5/9/6/

[4] SEMI, " Definition of Measurement Index (Semu) for Luminance Mura in FPD Image Quality Inspection," SEMI D31-1102, 2002.

[5] [VESA, "Flat Panel Display Measurements Standard Ver. 2.0," June 1, 2001 2001.

[6] [Y. Mori, K. Tanahashi, and S. Tsuji, "Quantitative evaluation of ``mura" in liquid crystal displays," *Optical Engineering*, vol. 43, pp. 2696-2700, 2004.

[7] B. C. Jiang, C.-C. Wang, and H.-C. Liu, "Liquid crystal display surface uniformity defect inspection using analysis of variance and exponentially weighted moving average techniques," *International Journal of Production Research*, vol. 43, pp. 67-80, 2005.

[8] K. Oka, K. Kitagishi, and Y. Enami, "Motion Artifacts Measured by Using a Pursuit Camera," presented at IDMC, Taipei, Taiwan, 2005.